arXiv:hep-ph/0104192v1 19 Apr 2001

Truncated BFKL Series in Electron-Proton Collisions

M.B. Gay Ducati and M.V.T. Machado

Instituto de Física, Univ. Federal do Rio Grande do Sul. Caixa Postal 15051, 91501-970 Porto Alegre, RS, BRAZIL.
E-mail: `gay@if.ufrgs.br`, `magnus@if.ufrgs.br`

ABSTRACT: We study the contribution of the truncated BFKL Pomeron series to the electroproduction process showing that a reliable description is obtained taking into account two orders in perturbation theory. Using the recent F_2 logarithmic slope data as a constraint to the adjustable parameters, the inclusive structure function is described in a wide range of the small x HERA kinematical region, consistent with the unitarity bound. We also extrapolate the predictions to the THERA region.

KEYWORDS: Diffractive physics; Perturbative calculations; BFKL dynamics..

1. Introduction

Deep inelastic electron-proton scattering experiments at HERA have provided measurements of the inclusive structure function $F_2(x, Q^2)$ in very small Bjorken variable x (10^{-2} down to 10^{-5}) [1]. In these processes the proton target is analysed by a hard probe with virtuality $Q^2 = -q^2$, where $x \sim Q^2/2p.q$ and p, q are the four-momenta of the incoming proton and the virtual photon probe. In that kinematical region, the gluon is the leading parton driving the small x behavior of the deep inelastic observables. The small x region is described in a formal way using the summation of gluon ladder diagrams, whose virtual contributions lead to the gluon reggeization [2]. Such ladders diagrams are associated with the Pomeron, a Reggeon with the vacuum quantum numbers, which was introduced phenomenologically to describe the high energy behavior of the total and elastic cross-sections of the hadronic reactions [3] and connected with the existence of large rapidity gaps in the produced final state [4].

In leading order (LO) all powers of $\alpha_s \ln(Q^2/\mu^2)$, with μ^2 the factorization scale, are summed by the DGLAP evolution equations [5], which take into account only the strongly ordered parton transverse momenta (k_T) ladders. At present the next-to-leading order (NLO) contribution is also used, including non-ordered k_T contributions in a covariant way [6]. In the current HERA kinematical regime the DGLAP approach is quite successfull, although the theoretical expectation of deviations due to the parton saturation phenomena should be present [7]. Further, corrections leading to non-linear evolution equation of the gluon distribution have been calculated in the literature [8, 9].

Moreover, at very small x the leading logarithms $\alpha_s \ln(1/x)$ are shown to be important [10]. In the leading logarithmic approximation (LLA) the QCD Pomeron corresponds to the sum of ladder diagrams with reggeized gluons along the chain, which are strongly ordered in momentum fraction x. Such sum is described by the Balitzkij-Fadin-Kuraev-Lipatov (BFKL) equation [10]. The corrections at next-to-leading level (NLLA) are now known, leading to strong modifications in the LLA spectrum [11]. Although some existing reasonable direct comparison with data [12], the BFKL approach presents the diffusion phenomena on momentun transfer ($\ln k_T$), which turns out the description of the inclusive observables as the structure function F_2 unreliable [13]. This comes from the fact that the diffusion leads to an increasingly large contribution from the infrared and ultraviolet regions of the transverse momenta k_T where the BFKL is not expected to be valid.

An important characteristic present at both DGLAP and BFKL approaches is that their solutions grow like a power of the center of mass energy s, therefore violating the unitarity bound at very high energies. This is one of the major problems of small x physics, since the Froissart-Martin bound states that the total cross section should not rise faster than $\sim \ln^2(s)$ at asymptotic high energies [14]. In the DGLAP approach, the unitarity problem requires corrections to give rise to the saturation

[15, 16] (taming the growth of the gluon distribution), while in the BFKL approach this difficulty can be surpassed considering the resum of all multiple BFKL Pomeron (calculated at LO) exchanges in the total cross section (and structure function) [17].

In this scenario, since the BFKL approach is asymptotic itself we have proposed that a truncated BFKL series was used to describe both total and differential cross section in hadronic collisions, namely proton-(anti)proton reactions [18]. In the atainable energies there is no room on pseudorapidity to enable a completely resummed n-rung ladder and studies have reported a strong convergence of the BFKL series considering few orders in the expansion [19]. Furthermore, it was found in [19] important evidence that the asymptotic solution to the BFKL equation is inappropriated in the most of the HERA range, and the expansion order by order allows to identify the onset of the region where the full BFKL series resummation is required.

The resulting scattering amplitude in Ref. [18] is consistent with the unitarity bound and obtained by just two orders on perturbation theory. The first term in the expansion (Born level) corresponds to the two reggeized gluon exchange leading to a constant (s-independent) contribution to the total cross section. The second term comes from the one rung gluon ladder and provides a logarithmic enhancement to the cross section. These two contributions are enough to describe successfully the acellerator data, and even the cosmic ray measurements. The distribution in momentum transfer t, namely the elastic differential cross section, is obtained taking into account the non-forward amplitude. It was shown in [18] the importance of a reliable phenomenological input for the proton impact factor, i.e., the coupling of the ladder to the proton vertex. A remarkable result in [18] is that the factorizable character in energy s and momentum transfer t presents in the non-forward amplitude allows an overall parametrization for the slope $B(s)$. This result is independent of the details about the Pomeron-proton coupling and holds by requiring that the amplitude is finite at t equal zero. Further, a phenomenological analyzes to the diffraction cone data of $pp(\bar{p})$ scattering has been made considering those ideas [20], corroborating our calculations.

Such good results in the hadronic sector motivate the analyzes of reliability at electron-proton collisions, focusing the small x region. In this work we sum two terms of the perturbative series in order to obtain the imaginary part of the DIS amplitude, and through the Optical theorem the inclusive structure function $F_2(x, Q^2)$. Using the latest HERA data (H1 and preliminary ZEUS) on F_2-logarithmic slope [21] to constrain the remaining parameters at the small x region, we perform a broadly description (no free parameter) of the structure function in the kinematical range of $10^{-5} < x < 10^{-2}$ and $0.35 < Q^2 < 150$ GeV^2. We analyse the resulting predictions for the upcoming THERA project, confronting them with the unitarity bound for this observable and compare the present approach to the complete BFKL series, which we treat later on.

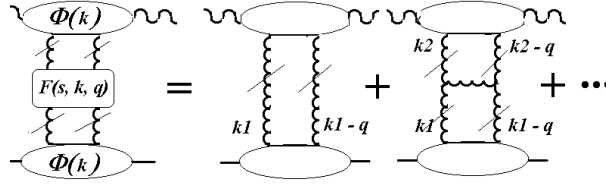This paper is organized as follows. In the next section one introduces the main

Figure 1: The upper blob denotes the virtual photon impact factor, the lower one represents the proton impact factor and the first two orders in perturbation theory are shown. In LLA, the ladder is constructed with reggeized gluons in the t-channel and bare gluons on the s-channel (the rungs), which are connected by a non-local gauge-invariant effective vertex (the bold blob).

formulae and the results for the inclusive structure function. In the Sec. (3), we calculate the observable $dF_2/d\ln Q^2$, and perform a fit to the updated HERA data on F_2-slope, determining the values of the existing parameters. As a consequence, the inclusive structure function is obtained straightforwardly and compared with the HERA small x results. The extrapolation into the THERA kinematical regime is performed in the Sec. (4). In the last section we draw our conclusions.

2. Small-x DIS in Perturbation Theory

In the center of mass frame, the deep inelastic lepton-nucleon scattering process is depicted as the scattering of the incoming lepton through a large angle, which radiates a highly virtual photon γ^*. The photon then scatters inelastically off the incoming nucleon (proton). The total cross section for the process $\gamma^* p \to X$, with X meaning all possible final states, is obtained via Optical theorem from the imaginary part of the elastic $\gamma^* p \to \gamma^* p$ amplitude (see Fig. 1). For high $\gamma^* p$ center of mass energies the BFKL approach is indicated to compute this cross section [22].

Now let us define the kinematics for the DIS process. The incoming electron and proton four-momenta are l and p, respectively, and the virtual space-like photon has a four-momentum q. The main kinematic invariants are given by

$$Q^2 = -q^2, \qquad s = (p+l)^2, \qquad W^2 = (p+q)^2, \qquad x = \frac{Q^2}{2p.q} \approx \frac{Q^2}{Q^2 + W^2}. \quad (2.1)$$

The last expression for x is correct in the limit of negligible electron and proton masses; the high energy region $W^2 >> Q^2$, which implies $x << 1$, defines the small x regime. The proton inclusive structure function and the longitudinal structure function can be written in terms of the cross sections for the scattering of transverse or longitudinal polarized photons in the form

$$F_2(x, Q^2) = \frac{Q^2}{4\pi^2\alpha} \left[\sigma_T(x, Q^2) + \sigma_L(x, Q^2)\right] , \qquad (2.2)$$

$$F_L(x, Q^2) = \frac{Q^2}{4\pi^2\alpha}\sigma_L(x, Q^2) . \qquad (2.3)$$

Then the structure functions are obtained computing the imaginary part of the amplitude for elastic $\gamma^* p$ scattering considering each photon polarization. In the asymptotic high energy limit, for photons with polarization δ, the cross section is the following [22]

$$\sigma_\delta(x, Q^2) = \frac{\mathcal{G}}{(2\pi)^4} \int \frac{d^2\mathbf{k_1}}{\mathbf{k_1}^2} \frac{d^2\mathbf{k_2}}{\mathbf{k_2}^2} \, \Phi_\delta^{\gamma^*}(\mathbf{k_1}) \, F(x, \mathbf{k_1}, \mathbf{k_2}) \, \Phi_p(\mathbf{k_2}) \qquad (2.4)$$

Here, $\mathcal{G}$ is the color factor for the color singlet exchange and $\mathbf{k_1}$ and $\mathbf{k_2}$ are the transverse momenta of the exchanged gluons in the t-channel (see Fig. 1). The $\Phi_\delta^{\gamma^*}(\mathbf{k_2})$ is the virtual photon impact factor (with $\delta = T, L$) and $\Phi_p(\mathbf{k_1})$ is the proton impact factor. These quantities correspond to the upper and lower blobs in the Fig (1), respectively.

The impact factors $\Phi(\mathbf{k})$, describing the interacting particles transition in the particle-Reggeon (i.e, Reggeons meaning the reggeized gluons) processes are, by definition, factorized from the Green's function for the Reggeon-Reggeon scattering $F(x, \mathbf{k_1}, \mathbf{k_2})$. As a consequence, the energy dependence is determined by this function, remembering that the center of mass energy of the system $\gamma^* p$ is W^2 and that $x \approx Q^2/W^2$. The BFKL kernel $F(x, \mathbf{k_1}, \mathbf{k_2})$ states the dynamics of the process and is completely determined in perturbative QCD. For example, the cancelation of the infrared singularities in the kernel is known from Ref. [23]. In addition, the amplitude describing the interaction of the particles (colorless) is the convolution of the kernel with the corresponding impact factors and it is infrared safe. Moreover, the infrared singularities cancelation in the impact factor of colorless particles has been demonstrated to next-to-leading order in Ref. [24].

The main properties of the LO kernel are well known [10] and the results arising from the NLO calculations suggest that the pQCD Pomeron can acquire very significant non-leading corrections, which have yielded intense debate in the current literature [11]. The main characteristic at LO is that the leading eingenvalue of the kernel leads to a strong rise with decreasing x, $F(x) \sim \frac{x^{-\varepsilon}}{\sqrt{\ln 1/x}}$, where $\varepsilon = 4\overline{\alpha}_s \ln 2 \approx 0.5$. As a consequence, the inclusive structure function has this same growth at low x.

Therefore, the resulting amplitude (i.e. total cross section and structure function) clearly violates the unitarity bound.

Instead of using the full BFKL series, we claim that a reliable description can be obtained considering its truncation up to two orders in the perturbative expansion. The arguments for this working hypothesis were already discussed in the introduction but we recall them here. Such procedure has been successfull into describing the hadronic cross sections in a consistent way concerning the unitarity constraint [18] and may be considered in the electroproduction case. The justification is that in the current acellerator domain the asymptotic regime was not reached and there is no room in rapidity to enable an infinite n-gluon cascade, represented diagrammatically by the BFKL ladder. Indeed, a steep convergence of the BFKL series in few orders in the perturbative expansion has been reported [19] and phenomenological studies indicate that such a procedure is reasonable at least in proton-proton collision [25]. In order to continue, we need to take into account the convolution between the impact factors and the corresponding gluon ladder exchanges in each order. The typical diagram for the DIS amplitude at small x in the lowest order in perturbation theory is depicted in Fig. (1). At the leading order the amplitude at high energies is purely imaginary and written at $t = 0$ as

$$\mathcal{A}^{Born}(W, t = 0) = \frac{2 \, \alpha_s \, W^2}{\pi^2} \sum_f e_f^2 \int \frac{d^2 \mathbf{k_1}}{\mathbf{k_1}^4} \, \Phi_\perp^{\gamma^*}(\mathbf{k_1}) \, \Phi_p(\mathbf{k_1}) \qquad (2.5)$$

and the next order in perturbation theory calculated at LLA yields

$$\mathcal{A}^{NO}(W, t = 0) = \frac{6 \, \alpha_s^2 \, W^2}{8 \, \pi^4} \sum_f e_f^2 \, \ln(W^2/W_0^2) \int \frac{d^2 \mathbf{k_1}}{\mathbf{k_1}^4} \frac{d^2 \mathbf{k_2}}{\mathbf{k_2}^4} \, \Phi_p(\mathbf{k_1}) \, K(\mathbf{k_1}, \mathbf{k_2}) \, \Phi_\perp^{\gamma^*}(\mathbf{k_2}) \, ,$$

where the α_s is the strong coupling constant, which is fixed in the LO BFKL approach. The running of the coupling constant contributes significantly for the NLO BFKL, since it is determined by subleading one-loop corrections, namely the self-energy and vertex-correction diagrams. The W_0 is the typical energy of the process, scaling the logarithm of energy and take an arbitrary value in LLA.

The function $K(\mathbf{k_1}, \mathbf{k_2})$ is the BFKL kernel at $t = 0$ and describes the gluon ladder evolution in the LLA of $\ln(s/t)$ as already discussed above. The Pomeron is attached to the off-shell incoming photon through the quark loop diagrams, where the Reggeized gluons are attached to the same and to different quarks in the loop [26] (see Fig. 2). The $\Phi_\perp^{\gamma^*}$ is the virtual photon impact factor averaged over the transverse polarizations [27]

$$\Phi_\perp^{\gamma^*}(\mathbf{k_2}) = \frac{1}{2} \int_0^1 \frac{d\tau}{2\pi} \int_0^1 \frac{d\rho}{2\pi} \frac{\mathbf{k_2}^2(1 - 2\tau\tau')(1 - 2\,\rho\rho')}{\mathbf{k_2}^2 \rho\rho' + Q^2 \rho \, \tau\tau'} \, , \qquad (2.6)$$

with ρ, τ the Sudakov variables associated to the photon momenta and the notation $\tau' = (1 - \tau)$ and $\rho' = (1 - \rho)$ is used.

The diagrams at LO for the photon impact factor are shown in the Fig. (2). The average over longitudinal polarization gives a smaller contribution to the total cross section (and F_2), and by simplicity it will be disregarded.

Although the BFKL approach is known at next-to-leading level [11], the impact factors are not yet determined at this order of perturbatiove expansion. Recently, it has been reported the effect of the so called exact kinematics of the exchanged gluons, which would give the most important contributions to the higher order terms [28].
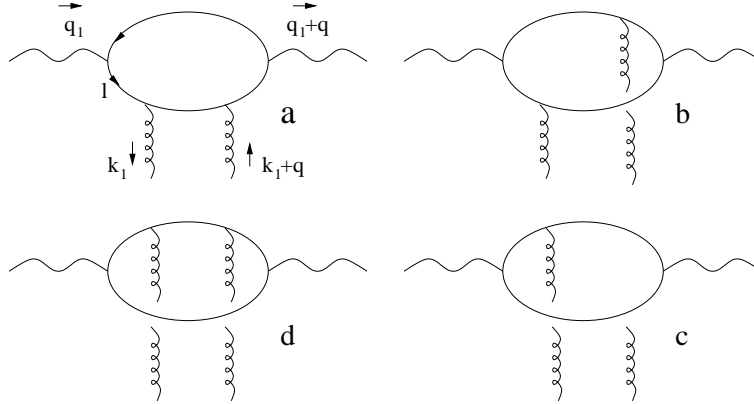

Figure 2: The diagrams contributing to the virtual photon impact factor at LO, from [26].

We are unable to compute the proton impact factor $\Phi_p(\mathbf{k_1})$ using perturbation theory since it is determined by the large-scale nucleon dynamics. A study has been performed at Ref. [29], where the solutions of the Lipatov equation are critically examined and their importance on the structure function description is determined using physically motivated modifications for small $\mathbf{k}^2$. Namely, it was performed a detailed parametrization of the infrared region which satisfies the gauge invariance constraints when $\mathbf{k}^2 \to 0$. Due to this gauge invariance $\Phi_p(\mathbf{k_1} \to 0) \to 0$, and it can be modeled as a phenomenological input by the expression

$$\Phi_p(\mathbf{k_1}) = \mathcal{N}_p \frac{\mathbf{k_1}}{\mathbf{k_1} + \mu^2} \tag{2.7}$$

where $\mathcal{N}_p$ is the unknown normalization of the proton impact factor and μ^2 is a scale which is typical of the non-perturbative dynamics. Such scale is related to the radius of the gluonic form factor of the proton. Considering it as the scale of the hadronic electromagnetic form factor, then $\mu^2 \simeq 0.5$ GeV^2 instead of estimates from QCD sum rules giving $\mu^2 \simeq 1 - 2$ GeV^2 [29].

When considering the photoproduction case there is no need to deal with both a specific form for the impact factors and the transverse momentum integration in the amplitudes. This allows to consider W-independent factors in each term as free
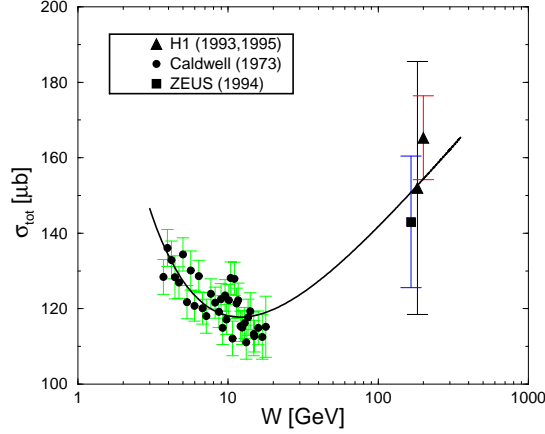
Figure 3: The result for the photoproduction cross section using the truncated BFKL series compared with the data [31].

parameters and to obtain them from data on photoproduction. In fitting these data, the Pomeron contribution described above should be added through a small non-diffractive component arising from the leading meson exchange trajectory. This is considered to be given by the phenomenological Donnachie-Landshoff form [30] (first term in the equation below). Then the expression for the photoproduction total cross section is

$$\sigma_{tot}^{\gamma^* p} = C_R \left(W^2/W_0^2\right)^{-0.4525} + C_{Born} + C_{NO} \ln(W^2/W_0^2) \,. \tag{2.8}$$

where $W_0^2 = 1$ GeV^2 (fixed), $C_R = 0.216$ mb, $C_{Born} = 0.044$ mb and $C_{NO} = 0.01$ mb. The result is shown in the Fig. (3) with the cross section data [31].

In the electroproduction case, using the Optical theorem and summing the two orders in perturbation theory we can write the expression for the inclusive structure function, following [27]

$$F_2(x, Q^2) = \frac{8}{3} \frac{\alpha_s^2}{\pi^2} \sum_f e_f^2 \, \mathcal{N}_p \left(I_{Born}(Q^2, \mu^2) + \frac{3 \, \alpha_s}{\pi} \ln\left(\frac{x_0}{x}\right) \, I_{NO}(Q^2, \mu^2) \right) \,, \tag{2.9}$$

where the functions $I_{Born, NO}(Q^2, \mu^2)$ are given by

$$I_{Born}(Q^2, \mu^2) = \frac{1}{2} \ln^2\left(\frac{Q^2}{\mu^2}\right) + \frac{7}{6} \ln\left(\frac{Q^2}{\mu^2}\right) + \frac{77}{18} \,, \tag{2.10}$$

$$I_{NO}(Q^2, \mu^2) = \frac{1}{6} \ln^3\left(\frac{Q^2}{\mu^2}\right) + \frac{7}{12} \ln^2\left(\frac{Q^2}{\mu^2}\right) + \frac{77}{18} \ln\left(\frac{Q^2}{\mu^2}\right) + \frac{131}{27} + 2 \, \zeta(3) \,.$$

Here, the x_0 gives the scale to define the logarithms of energy for the LLA BFKL approach and $\zeta(3) = \sum_r (1/r^3) \approx 1.202$ is the Riemann ζ-function. It was verified

in [27] that the coefficients in front of the logarithms of virtuality Q^2, which are determined by the anomalous dimensions of twist-2 operators (OPE), coincide up to the factor $2/3$. Also the subsequent two terms in the expansion, corresponding to the contributions of order $\alpha_s^2 \ln^2(1/x)$ and $\alpha_s^3 \ln^3(1/x)$, are calculated.

Some comments about the result above are in order. The high energy or Regge-limit for the virtual photon-proton scattering is connected with the behavior of the structure function $F_2(x, Q^2)$ when x goes to very small values ($x \to 0$). The main approaches to describe the Regge limit are based on QCD perturbation theory [5,10], and both predict a rise of the structure function at large Q^2 and small x. However, one expects [7] this rise of the cross section at large energies to be tamed by screening corrections leading to an asymptotic behavior required by the Froissart bound [14]. The result for F_2 in our calculations is obtained taking into account this unitarization requirement *a priori*.

Concerning the Regge phenomenology, the truncated BFKL series presents the main characteristics of the Regge-Dipole Pomeron model (see, for instance [33]). Namely, in the Dipole Pomeron $F_2(x, Q^2) \sim R(Q^2) \ln(1/x)$ and this behavior corresponds to the contribution of a double j-pole to the partial amplitude of $\gamma^* p \to \gamma^* p$, where $R(Q^2)$ is the residue function of the Pomeron. The resultant trajectory has unit intercept, $\alpha_{I\!P}(0) = 1$.

Also it is interesting to compare the resultant structure function with the complete perturbative expansion. Indeed, Navelet et al. [34] have taken into account the full BFKL series described in the QCD dipole picture. Using the k_T-factorization properties of high energy hard interactions the proton structure function is obtained in a 3-parameter expression, which gives a fair description of H1 data at $Q^2 \le 150$ GeV^2. It is written as

$$F_2^{BFKL}(x, Q^2) = \mathcal{N} \, a^{1/2} \exp^{(\alpha_{I\!P}-1)\ln\left(\frac{1}{x}\right)} \left(\frac{Q}{Q_0}\right) \exp^{-\frac{a}{2}\ln^2\left(\frac{Q}{Q_0}\right)} \qquad (2.11)$$

There, $a = \left(\frac{\bar{\alpha}_s N_c}{\pi} 7 \zeta(3) \ln(1/x)\right)^{-1}$, and $\alpha_{I\!P} = 4 \bar{\alpha}_s N_c \ln 2/\pi + 1$ is the BFKL Pomeron intercept. The parameters are $\mathcal{N} = 0.077$, $Q_0 = 0.627$ and $\alpha_{I\!P} = 1.282$ (corresponding to an effective coupling constant $\bar{\alpha}_s \simeq 0.11$). Moreover, in Ref. [35] the DLA limit of BFKL in the dipole picture was calculated and it was shown that the transition region between these two approaches is $Q^2 \approx 150$ GeV^2, i.e. this is the domain where the LO BFKL Pomeron states. Later, we turn out to the Navelet et al. result in our predictions to the THERA kinematical region, when one compares both the truncated and the full BFKL series in that domain.

As a remark, we notice that the expression (2.9), consistent with the unitarity limit, gives some theoretical fundamentation to the existing study regarding scaling properties in deep inelastic scattering [32]. It was found that the available data on small x regime are well described by a polinomial linear in $\ln(1/x)$ for every measured

Q^2-value, $F_2(x, Q^2) = u_0(Q^2) + u_1(Q^2) \log \frac{\nu(Q^2)}{x}$, where possible higher order terms in $\log(1/x)$ are statistically non significant [32].

Now, having the expression for the inclusive structure function, in the next section we compare it with the HERA experimental results, determining the adjustable parameters and the range of validity from this model.

3. Comparison with the HERA experiment

Now we proceed to compare the expression obtained for the inclusive structure function $F_2(x, Q^2)$ with the truncated BFKL series with the experimental results. We choose to use a smaller data set defined by the latest HERA experimental measurements of the Q^2 logarithmic derivative of F_2, which lies in the small x region $x < 10^{-2}$. These updated data on the slope are precise enough to determine unambiguously the two phenomenological non-perturbative parameters $\mathcal{N}_p$, μ^2 and the scale x_0.

Before to perform the analyzes, we should discuss the main features of the slope data. The global analyzes of the proton structure function data do not present significant deviations from DGLAP approach, however measurements of the rate of change of the logarithmic Q^2 dependence of F_2, i.e. the Q^2-slope, have shown possible deviations from the expected pQCD behavior at small x and small Q^2. These results may be interpreted as signal of unitarity corrections, namely that the system has reached to a QCD regime of gluon saturation [36, 37]. Such effects can be analyzed in that quantity, since in leading order DGLAP evolution it is directly proportional to the gluon structure function $xG(x, Q^2)$ [38],

$$\frac{\partial F_2(x, Q^2)}{\partial \ln Q^2} = \frac{2 \alpha_s}{9 \pi} xG_{DGLAP}(x, Q^2). \tag{3.1}$$

The most important experimental observation is that at fixed x the slope is a monotonic decreasing function of the virtuality Q^2. For fixed Q^2 it increases as x becomes smaller. In the reference [37], it was verified that the Q^2-slope behavior as measured in the kinematic region currently available at HERA does not present unambiguous signs of saturation. Indeed, this observable can be described by the usual DGLAP formalism considering the latest parton distribution or DGLAP with saturation effects as well as by some Regge based models. The procedure to distinguish between models for gluon saturation and the Regge inspired ones (including soft and hard interactions) is not an easy task because the saturation scale $Q_s(x) \sim 1 - 5$ GeV^2 (setting the virtuality where unitarity effects start to be visible) at the current HERA domain occours at similar values of the matching of the soft and hard components. Indeed, concerning this question we have proposed the logarithmic slope from the diffractive structure function as a potential observable to distinguish such dynamics [39].
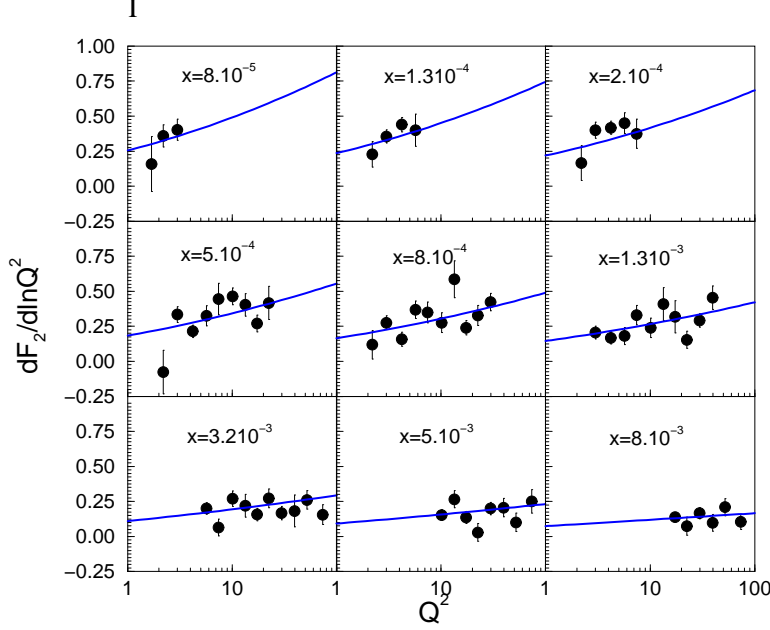
Figure 4: The result for the partial derivative $\partial F_2/\partial \ln Q^2$ plotted as a function of Q^2 (in GeV^2) for fixed x, using the truncated BFKL series compared with the latest H1 data [21]. The errors are summed in quadrature.

Considering the truncated BFKL series, the F_2-slope can be calculated straightforwardly from Eq. (2.9), yielding

$$\frac{\partial F_2(x, Q^2)}{\partial \ln Q^2} = \frac{4}{3} \frac{\alpha_s^2}{\pi^2} \sum_f e_f^2 \mathcal{N}_p \left[2 \ln \left(\frac{Q^2}{\mu^2} \right) + \frac{14}{6} + \right.$$

$$\left. + \frac{3 \, \alpha_s}{\pi} \ln \left(\frac{x_0}{x} \right) \left(\ln^2 \left(\frac{Q^2}{\mu^2} \right) + \frac{7}{3} \ln \left(\frac{Q^2}{\mu^2} \right) + \frac{77}{9} \right) \right] \qquad (3.2)$$

The above theoretical result is compared with the current HERA data for the logarithmic slope. A combination of the published H1 data and the preliminary ZEUS ones [21] is used. Both sets of experimental data allow to cover a kinematical range corresponding to virtualities of $0.3 < Q^2 < 40$ GeV^2 and Bjorken variable of $10^{-5} < x < 10^{-2}$.

In the Fig. (4) we show the result for the H1 data on the Q^2-logarithmic derivative, considering the Q^2 dependence at fixed x. A reasonable description is obtained for the measured kinematical range. The resultant parameters are shown in the Table 1. We noticed that to consider the strong coupling constant as a free parameter does not improve the description, therefore one considers it fixed, namely $\alpha_s = 0.2$. The overall normalization is defined as $\mathcal{N} = \frac{4}{3} \frac{\alpha_s}{\pi^2} \sum e_f^2 \mathcal{N}_p$, depending on non-perturbative physics through the normalization of the proton impact factor $\mathcal{N}_p$.

Although the quite different expression for the dependence on the virtuality (see Eq. 3.2), our approach provides a similar shape as the parametrization linear in $\ln Q^2$

DATA SET	$\mathcal{N}$	μ^2	x_0	α_s
H1 Collaboration	0.009	0.068	0.008	0.2 (fixed)

Table 1: The parameters from the H1 data on the Q^2-logarithmic derivative [21] ($\chi^2 = 0.01$).
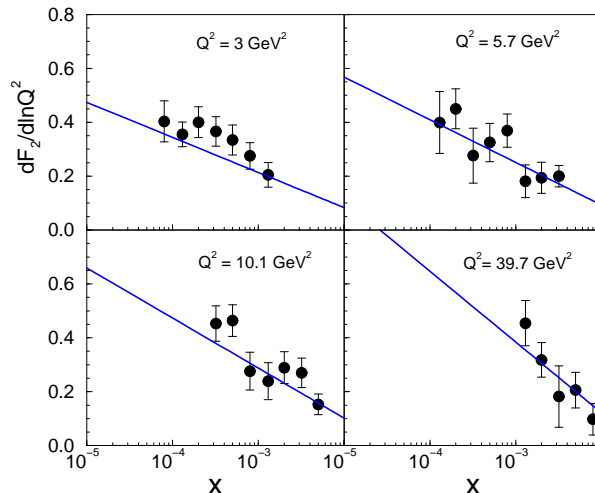

Figure 5: The result for the partial derivative $\partial F_2/\partial \ln Q^2$ plotted as a function of x for fixed virtualities $Q^2 = 3$, 5.7, 10.1, 39.7 GeV^2, using the truncated BFKL series compared with the latest H1 data [21]. The errors are summed in quadrature.

employed by the H1 Collaboration in the data analyzes [21]. The value found for the scale $\mu = 0.26$ GeV is consistent with a non-perturbative input, i.e. $\mu \sim \Lambda_{QCD} \approx 0.2$ GeV. The parameter x_0, which provides the scale to define the logarithms on energy and the region where the dynamics of the LLA summation is suitable, lies in the small x domain, $x \ll x_0 \approx 10^{-2}$.

The dependence on x for the logarithmic slope is presented in Fig. (5), at fixed representative virtualities. The model describes broadly the data in the range considered. An important feature of the approach is a attenuated increasing of the gluon distribution at low x [see Eqs. (3.1-3.2)], observed in the plots through the extrapolations into smaller momentum fraction values. The DGLAP evolution equation, instead provides a stronger and continuous rise towards small x for fixed Q^2 [21].

In the Fig. (6) we show the result for the preliminary ZEUS data on the logarithmic slope versus Q^2, at fixed momentum fraction x . The data points were taken from the plots of [21]. We determined the adjustable parameters from this data set, however it should be stressed the preliminary character of this result. The values are shown in Table (2).

The values obtained are consistent with those found from the H1 data set. The main feature of the ZEUS experimental measurement is the presence of points ob-

DATA SET	$\mathcal{N}$	μ^2	x_0	α_s
ZEUS Coll. (preliminary)	0.006	0.053	0.0053	0.2 (fixed)

Table 2: The parameters from the ZEUS preliminary data on the Q^2-logarithmic derivative [21].
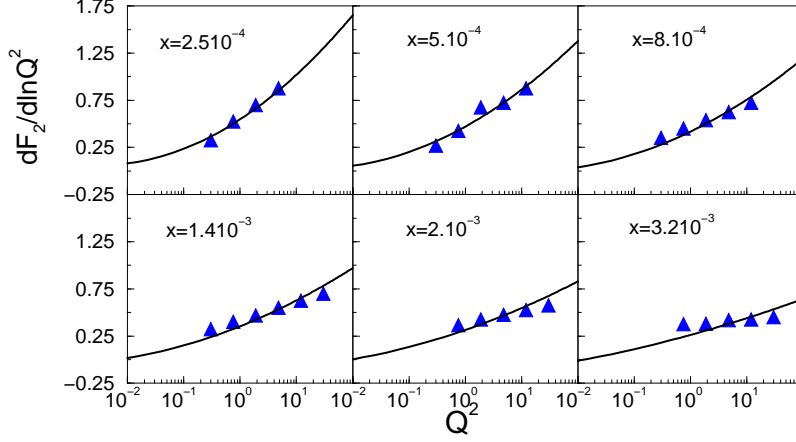

Figure 6: The result for the partial derivative $\partial F_2/\partial \ln Q^2$ plotted as a function of Q^2 (in GeV^2) for fixed x, using the truncated BFKL series compared with the latest preliminary ZEUS data. The points were taken from the plots of [21].

tained at very low virtualities $Q^2 \geq 0.3$ GeV^2. The plots present the same characteristics as the H1 data set, for instance, a linear behavior in $\ln Q^2$ is observed. We notice that the ZEUS Collaboration parametrized the slope data with the expression $\frac{\partial F_2}{\partial \log_{10} Q^2} = B + C \log_{10} Q^2$. In our analyzes we converted the data points to $\ln Q^2$, similarly to those taken from H1.

Having the parameters determined from the fit to the Q^2-slope data, we use our expression for the inclusive structure function $F_2(x, Q^2)$ to determine the region of validity of the model considering the truncation of the BFKL series. The data set are separated, in the context of this paper, in the regions corresponding to low, medium and large virtualities, considering both H1 and ZEUS experimental results [40]. Here, one uses the parameters values obtained from H1 data set, since the analyzes are published. The first set analysed was the low Q^2 data in HERA collider. This kinematical domain has considerable importance since it is a region of transition between soft and hard physics. Namely, it defines the range where unitarity corrections should start to appear or the transition region for the matching of soft-hard contributions. The results are shown in the Figs. (7-8).
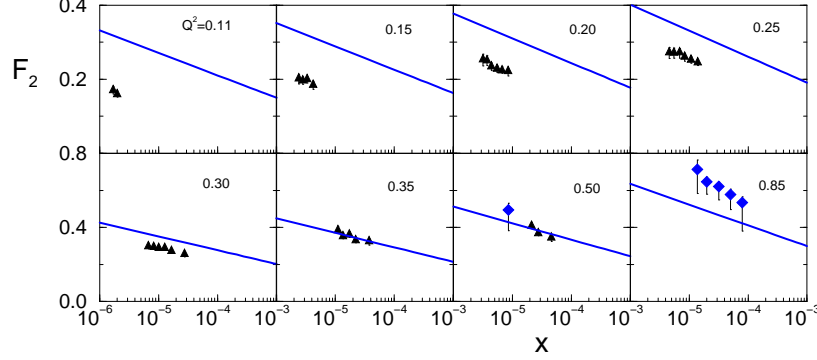
Figure 7: The estimates for the inclusive structure function at very small virtualities (in GeV^2) with the data of H1 (diamonds) and ZEUS (triangles up) [40].
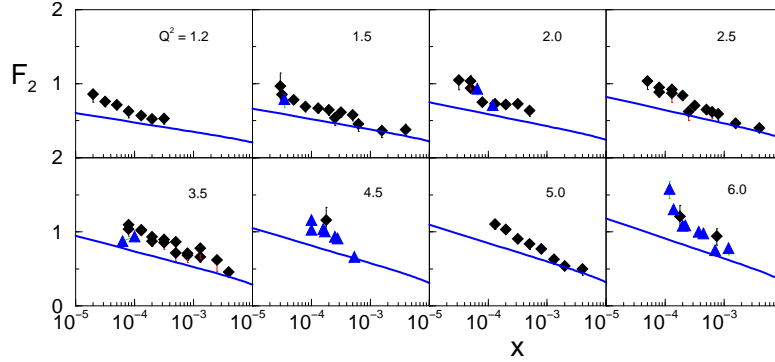

Figure 8: The estimates for the inclusive structure function at small virtualities (in GeV^2) with the data of H1 (diamonds) and ZEUS (triangles up) [40].

We notice that this is a prediction with no additional free parameter, all already determined from the slope data [see Tab. (1)]. A reasonable description is present starting at virtualities $Q^2 > 0.3$ GeV^2. For $Q^2 \geq 0.85$ GeV^2 the curve lies slightly below the data points. This fact is expected, since even that the main contribution at

small x should come from the perturbative Pomeron, a certain amount of background in the structure function due to quarks and non-perturbative effects (soft exchanges like the Donnachie-Landshoff Pomeron) should be taken into account [12]. It is noticeable also the partial agreement with the very low Q^2 measurements, where we would not expect such a good description.

The next set of data corresponds to the medium virtualities for the H1 and ZEUS measurements [40]. The result is shown in the Fig. (9-10). The truncated BFKL series describes reasonably the data in this kinematical range, except for excedingly larger x values ($x > 10^{-2}$). The curve still lies slightly below the data points, but with better accordance than the previous set. Deviations at greater x are expected, since we constraint our parameters from data belonging to $x < 10^{-2}$ and the reggeonic contribution should not be disregarded in this kinematical region.
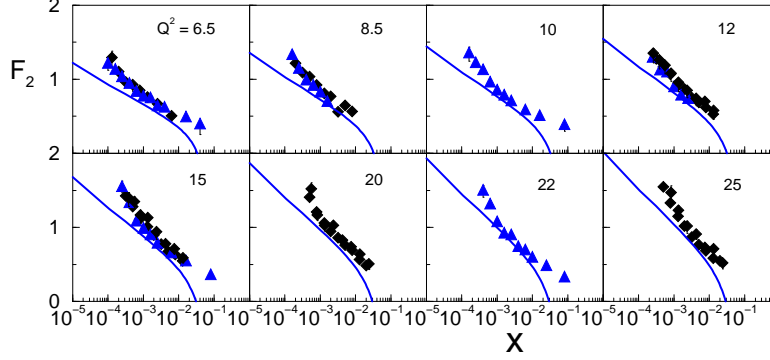
Figure 9: The result for the inclusive structure function at medium virtualities (in GeV^2) with the data of H1 (diamonds) and ZEUS (triangles up).
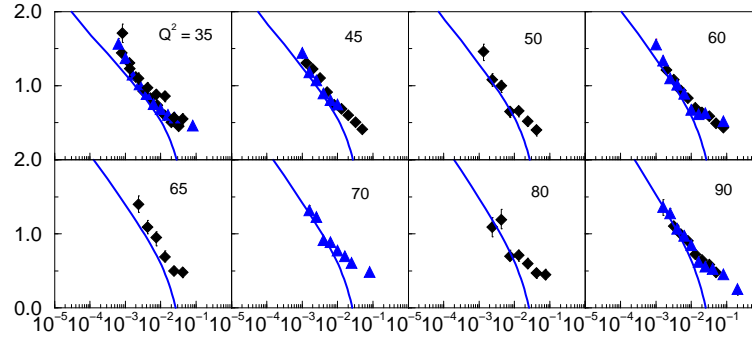

Figure 10: The result for the inclusive structure function at medium to high virtualities (in GeV^2) with the data of H1 (diamonds) and ZEUS (triangles up).

The last data set corresponds to the large virtualities range at HERA. The results are shown in the Fig. (11). The truncated BFKL series reproduces the data on $x < 10^{-2}$ quite well up to $Q^2 = 350$ GeV^2. The data set on large virtualities are dominated by data at large $x > 10^{-2}$, which we are unable to describe since this region is not dominated by the perturbative Pomeron. An improvement would be the introduction of the reggeonic piece, as discussed above.

Summarizing the results presented for the proton structure function:
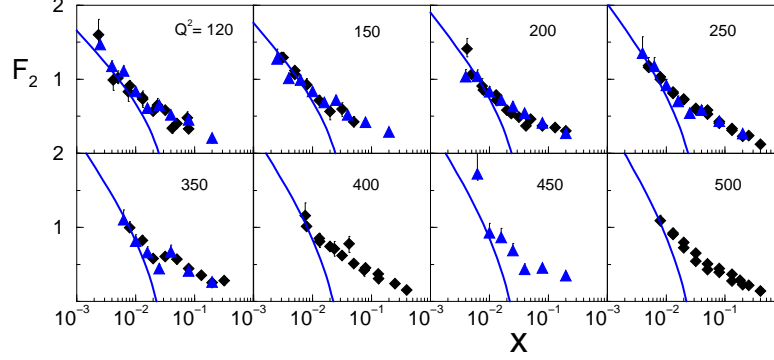
15

Figure 11: The result for the inclusive structure function at large virtualities (in GeV^2) with the data of H1 (diamonds) and ZEUS (triangles up).

- the truncated BFKL series up to second term allows to describe simultaneously the slope data and the F_2 in a wide kinematical regime. The description of the slope is in good agreement with the experimental results. Regarding the structure function F_2, agreement is obtained for the range $0.3 \leq Q^2 \leq 350$ GeV^2, considering the kinematical constraint $x \leq 10^{-2}$. If a such cut is not considered, the description is restricted in a smaller range of virtualities ($0.3 \leq Q^2 \leq 150$ GeV^2);

- the growth of $F_2(x, Q^2)$ presents large deviations from the steep increasing present at both the LO BFKL series and the DGLAP approach, where $F_2 \sim x^{-\lambda}$;

- there is room to include the contribution from non-perturbative sector (soft dynamics), mainly at low Q^2 virtualities. However it should be stressed that they are not big, namely we estimated that the correction corresponds to about 20 % to the overall normalization;

- the measurements at very large Q^2 lie often at $x > 10^{-2}$ where the approach is expected not to be valid and a reliable parametrization to the large x region should be introduced;

- we are not able to distinguish unambiguously the complete BFKL series [34] and the truncation up to second order, since both approaches describe the current HERA data. For instance, Navelet et al. and the present study produce a

16

broadly description of data at $1.5 \leq Q^2 \leq 150$ GeV^2. However, our analyzes extend the predictions to very low $Q^2 \sim 0.3$ GeV^2 and larger $Q^2 \geq 150$ GeV^2.

- a study of the sensitivity of summing an additional term in the perturbative expansion is required, and at this level the result should reach the asymptotic behavior $F_2 \sim \ln^2(1/x)$.

In the next section one uses the main results and conclusions obtained here, to make predictions to the forthcoming experiment THERA. We focus in the behavior of the complete BFKL series and its truncation in order to estimate the Q^2 logarithmic slope and the proton structure function in that kinematical domain.

4. The THERA kinematical Region

The upcoming THERA project [41], that will be realized at DESY as the successor of HERA, should use the electrons or positrons accelerated in the linear collider TESLA and the protons from HERA. THERA enables the energy frontier in deep inelastic physics to be raised up to about $\sqrt{s} \simeq 1$ GeV^2, allowing studies at virtualities Q^2 about 10^6 GeV^2 and Bjorken x down to 10^{-6} in the perturbative region. This future kinematical domain enables effectivelly to probe the saturation phenomena, since the saturation scale at THERA would be higher than the values found at HERA.

Our first study in the THERA kinematical region is to consider the logarithmic derivative, Eq. (3.2), versus the virtualities Q^2, considering the values of x planned to be available (see Fig. 12). This quantity can be compared with the unitarity bound for the Q^2-slope, which using the weak form of the unitarity constraint is expressed as [42]

$$\frac{\partial F_2(x, Q^2)}{\partial \ln Q^2} \leq \frac{Q^2 R^2}{3 \, \pi^2} , \qquad (4.1)$$

where the size of the target is $R^2 = 8.5$ GeV^{-2} [43].

We verify that our model does not violate strongly the unitarity bound, overestimating that limit at $Q^2 \simeq 2.5$ GeV^2 for $x = 10^{-6}$ and $Q^2 \simeq 3$ GeV^2 for $x = 10^{-7}$. Concerning the gluon saturation approaches, the intersection point between the usual DGLAP dynamics and the unitarity bound defines the saturation scale $Q_s(x)$. At HERA regime this scale lies in the same order of the models mixing soft and hard contributions. However, at THERA domain we expect to distinguish between these approaches [43]. Instead, in our case the violation of the unitarity bound informs us that at THERA regime there is enough energy to enable the emission of one more s-channel gluon in the BFKL ladder (two rungs) and one should include the next term of the perturbative expansion, resulting in $F_2 \sim \ln^2(1/x)$. We notice that such a contribution actually saturates the Froissart bound and the expansion should stop
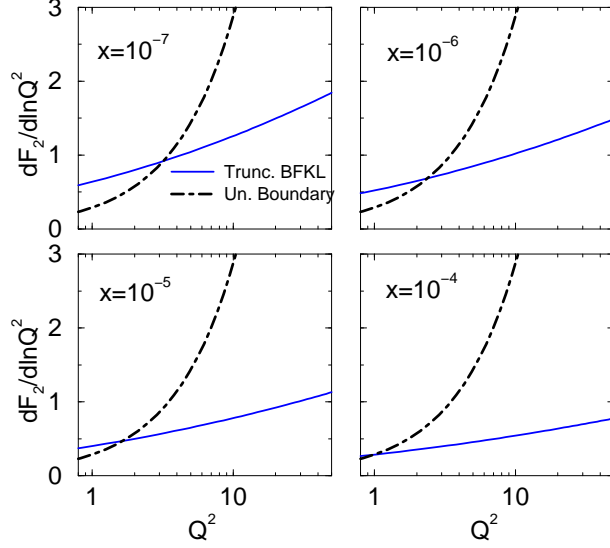
Figure 12: The prediction of the truncated BFKL series (solid lines) for the F_2-slope versus Q^2 compared with the unitarity limit (dot-dashed lines) in the THERA kinematical region.
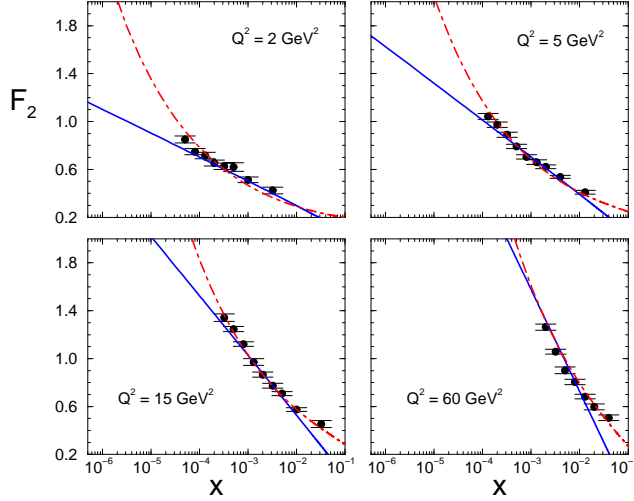

Figure 13: The prediction of the truncated BFKL series (solid lines) for the proton structure function versus x compared with the complete BFKL approach [34] (dot-dashed lines) extrapolated to the THERA kinematical domain.

at this level. In other words, the virtualities in which the unitarity bound is violated provide the threshold region where the present approach is applicable.

An important calculation is to estimate the proton structure function in the THERA region. Due to the quite different behavior for the gluon distribution predicted by the complete BFKL series and its truncation, we expect to distinguish the relevance of each additional order in the perturbative expansion using the kine-

matical domain to be realized at THERA. In Fig. (13), we present the structure function versus x at representative virtualities plotted with the latest H1 data for this observable [21], extrapolated up to momentum fraction $x = 10^{-7}$. As a remark, we have corrected the F_2 normalization from the truncated BFKL series multiplying it by a factor 1.2 to take into account the background effects (about 20 % in this domain).

An impressive deviation from the complete BFKL series, which takes into account the n-gluon emission cascade, have been found at very low x. The growth of the structure function, and implicitly of the gluon distribution, is softer than the solution from DGLAP evolution equation and of the BFKL-like models. The difference is stronger at lower virtualities, whereas at larger Q^2 both approaches are in better agreement. Such a result is already expected, since the most important region for saturation (unitarization) lies in the domain of small x and low Q^2. As a final comment, when the data from THERA are to be available the dynamics should be unambiguously distinguished. As a consequence, the observables depending directly from the gluon distribution, as F_L and charm structure function, are expected to give a signal for clear deviations from the conventional renormalization group evolutions, i.e. the DGLAP approach.

5. Conclusions

We study in detail the contribution of a finite sum of gluons ladders to the deep inelastic process, considering the truncation of the complete BFKL Pomeron series at the second order in the perturbative expansion $\alpha_s \ln(1/x)$. The main motivation is that in the present ep acellerator energies there is no phase space in rapidity $y = \ln(1/x)$ to enable a n-gluon ($n \rightarrow \infty$) emission cascade in the final state. An important and additional question is the violation of the unitarity bound in asymptotic energies from the current pQCD approaches, i.e. DGLAP and BFKL. The truncation provides a cross section unitarity safe, meaning that we are in a pre-asymptotic regime. One more term in the expansion may be added as the energy increases, which then should be enough at very high energies since $\sigma_{tot} \sim \ln^2(1/x)$, reaching the Froissart bound.

Using the truncated BFKL we are able to calculate the proton structure function and its Q^2 logarithmic derivative. The expressions are obtained with three adjustable parameters. Two of them came from the non-perturbative physics taking into account the modeling to the Pomeron-proton coupling; the $\mathcal{N}_p$ gives the normalization of the proton impact factor and the scale μ^2 is associated to the radius of the gluonic form factor of the proton. The energy scale x_0 provides the threshold region where the perturbative calculation is reliable, and a theoretical expectation is that it takes the value $x_0 \leq 10^{-2}$ (setting the small Bjorken x region and the domain of validity of the approach).

We choose to determine the parameters from a smaller data set, meaning the the latest HERA measurements on the Q^2 logarithmic derivative reported by the H1 and ZEUS Collaboration. The values found are consistent with the naive estimates, namely μ^2 lies in the non-perturbative domain ($\mu \approx \Lambda_{QCD}$) in both data sets and x_0 takes a value consistent with the Regge limit. The fitted expression to the slope describes this observable with good agreement, producing effectively the same linear behavior in $\ln Q^2$ considered by the H1 Collaboration experimental analyzes. Considering the x dependence of the slope, we obtain a gluon distribution softer than those coming from the usual approaches, $xG(x, Q^2) \sim x^{-\lambda}$, when one goes towards small x. The sensitivity in the growth of the gluon distibution at smaller momentum fraction taking the next order in the expansion is an interesting issue, however we postpone such analyzes for a future study.

Having the adjustable parameters obtained from the slope data, a parameter-free study of the proton structure function is performed. Agreement is obtained for the range $0.3 \leq Q^2 \leq 350$ GeV^2, considering the kinematical constraint $x \leq 10^{-2}$. If such a cut is not considered, the description is restricted into a smaller range of virtualities ($0.3 \leq Q^2 \leq 150$ GeV^2). The growth of the structure function presents large deviations from the steep increasing present at both the LO BFKL series and the DGLAP approach, where $F_2 \sim x^{-\lambda}$ as already discussed above. The non-perturbative contribution (from the soft dynamics), mainly at low Q^2 virtualities, is found to be small. Indeed, it was estimated that such effects introduces a correction of about 20 % in the overall normalization. We are not able to predict reliably the measurements at very large Q^2 , which lie often at $x > 10^{-2}$ and where the approach is expected not to hold. Moreover, the complete BFKL series and its truncation up to second order can not be distinguished unambiguously since both approaches describe the current HERA data. Nevertheless, our analyzes allowed to extend the estimates to very low virtualities $Q^2 \sim 0.3$ GeV^2 and larger $Q^2 \geq 150$ GeV^2.

The forthcoming THERA experiment opens a new kinematical window towards smaller x ($\sim 10^{-6}$) and higher virtualities. The predictions from the saturation models may be tested in this domain, determining if unitarity effects start to be important in the description of the main observables. The extrapolation of our results in the THERA region produced the following conclusions: the approach does not violate strongly the unitarity limit for the logarithmic slope. The region where this bound and the approach meet defines the domain of validity of the last one. Extrapolating the proton structure function down to momentum fraction $x \geq 10^{-7}$, remarkable deviations from the complete BFKL series have been found at very low x. The difference is stronger at lower virtualities, which allows to distinguish the relevance of each additional term in the expansion, when the data from THERA are to be avaluable.

Acknowledgments

References

[1] M. Klein. *Int. J. Mod. Phys.* **A15S1**, 467 (2000).

[2] L.N. Lipatov. in *Perturbative QCD*, ed. A.H. Mueller (World Scientific, Singapore, 1989).

[3] E. Predazzi, in International Workshop on Hadron Physics 98, edited by E. Ferreira, F. Cruz and S. Avancini, World Scientific, 1999, p. 80 [hep-ph/9809454].

[4] J.D. Bjorken. *Phys. Rev.* **D47**, 101 (1993).

[5] Yu.L. Dokshitzer. *Sov. Phys. JETP* **46**, 641 (1977);
G. Altarelli and G. Parisi. *Nucl. Phys.* **B126**, 298 (1977);
V.N. Gribov and L.N. Lipatov. *Sov. J. Nucl. Phys* **28**, 822 (1978).

[6] A. Vogt. *Nucl. Phys* (Proc. Suppl.) **B79**, 102 (1999).

[7] A.H. Mueller. *Small-x Physics, High Parton Densities and Parton Saturation in QCD*, [hep-ph/9911289].

[8] L.V. Gribov, E.M. Levin, M.G. Ryskin. *Nucl. Phys.* **B188**, 555 (1981); *Phys. Rep.* **100**, 1 (1983).

[9] A.L. Ayala, M.B. Gay Ducati, E.M. Levin. *Nucl. Phys* **B493**, 305 (1997); *Nucl. Phys* **B511**, 355 (1998).

[10] E.A. Kuraev, L.N. Lipatov and V.S. Fadin. *Phys. Lett* **B60** 50 (1975); *Sov. Phys. JETP* **44** 443 (1976); *Sov. Phys. JETP* **45** 199 (1977);
Ya. Balitsky and L.N. Lipatov. *Sov. J. Nucl. Phys.* **28** 822 (1978).

[11] V.S. Fadin, L.N. Lipatov. *Phys. Lett.* **B429**, 127 (1998) and references therein;
M. Ciafaloni. *Phys. Lett.* **B429**, 363 (1998);
G. Camici, M. Ciafaloni. *Phys. Lett.* **B430**, 349 (1998);
G.P. Salam. *Acta Phys. Pol.* **B30**, 3679 (1999);
M. Ciafaloni, D. Colferai, G.P. Salam. *Phys.Rev.* **D60**, 114036 (1999).

[12] J. Kwiecinski, A.D. Martin. *Phys. Lett.* **B353**, 123 (1995);
I. Bojak, M. Ernst. *Phys. Rev.* **D53**, 80 (1996).

[13] J.R. Forshaw, P.J. Sutton. *Eur. Phys. J.* **C1**, 285 (1998).

[14] M. Froissart. *Phys. Rev.* **123**, 1053 (1961).
A. Martin. *Phys. Rev.* **129**, 1462 (1963).

[15] K. Golec-Biernat, M. Wüsthoff. *Phys. Rev.* **D59**, 014017 (1999); *Phys. Rev.* **D60**, 114023 (1999).

[16] A. Ayala, M.B. Gay Ducati, V.P. Gonçalves, *Phys. Rev.* **D59** 054010 (1999).

[17] Y. Kovchegov. *Phys. Rev.* **D61**, 074018 (2000).

[18] M.B. Gay Ducati, M.V.T. Machado. *Phys. Rev.* **D63**, 094018 (2001); *Nucl. Phys.* (Proc. Suppl.) **B99**, 265 (2001).

[19] J.R.Forshaw, M.G.Ryskin. *Z. Phys.* **C68**, 137 (1995).

[20] K. Kontros, A. Lengyel, Z. Tarics. [hep-ph/0011398].

[21] H1 Collaboration. *Deep inelastic inclusive ep scattering at low x and a measurement of α_S*, preprint DESY-00-181 (to appear in *Eur. Phys. J.*), [hep-ex/0012053];
ZEUS Collaboration. *A study of scaling violations in the proton structure function F_2*, in 30th International Conference on High Energy Physics (ICHEP2000), Osaka, July (2000)[plenary session 12, paper 416].

[22] J.R. Forshaw, D.A. Ross. *QCD and the Pomeron.* Cambridge Press (1997).

[23] V.S. Fadin, L.N. Lipatov. *Phys. Lett.* **B429**, 127 (1998).

[24] V.S. Fadin, A.D. Martin. *Phys. Rev.* **D60**, 114008 (1999).

[25] R. Fiore *et al.* *Phys. Rev.* **D63**, 056010 (2001).

[26] N. G. Evanson, J. R. Forshaw. *Phys. Rev.* **D60**, 034016 (1999).

[27] I. Balitsky, E. Kuchina. *Phys.Rev.* **D62**, 074004 (2000).

[28] A. Bialas, H. Navelet, R. Peschanski. *Virtual photon impact factors with exact gluon kinematic*, [hep-ph/0101179].

[29] A.J. Askew, J. Kwieciński, A.D. Martin, P.J. Sutton. *Phys. Rev.* **D49**, 4402 (1994).

[30] A. Donnachie, P.V. Landshoff. *Phys. Lett.* **B296**, 227 (1992).

[31] D.O. Caldwell et al. *Phys. Rev* **D7**, 1362 (1973);
T. Ahmed et al. *Phys. Lett.* **B299**, 374 (1993);
M. Derrick et al. *Z. Phys.* **C63**, 391 (1994).
S. Aid et al. *Z. Phys.* **C69**, 27 (1995).

[32] W. Buchmüller, D. Haidt. *Double-logarithmic Scaling of the Structure Function F_2 at small x*, [hep-ph/9605428]
D. Haidt. *Nucl. Phys.* **B79** (Proc. Suppl.), 186 (1999).

[33] P. Desgrolard, A. Lengyel, E. Martynov. *Eur. Phys. J.* **C7**, 655 (1999).

[34] H. Navelet, R. Peschanski, Ch. Royon, S. Wallon. *Phys. Lett.* **B385**, 357 (1996).

[35] M.B. Gay Ducati, V.P. Gonçalves. *Phys. Lett.* **B437**, 177 (1998).

[36] M.B. Gay Ducati, V.P. Gonçalves. *Phys. Lett.* **B487**, 110 (2000); Erratum-ibid. **B491**, 375 (2000).

[37] E. Gotsman et al.. *Phys. Lett.* **B500**, 87 (2001).

[38] K. Pritz. *Phys. Lett.* **B332**, 393 (1994).

[39] M.B. Gay Ducati, V.P. Gonçalves, M.V.T. Machado. *Phys. Lett.* **B** (2001) (in press), [hep-ph/0010059].
M.B. Gay Ducati, V.P. Gonçalves, M.V.T. Machado. *The Logarithmic Slope in Diffractive DIS*, [hep-ph/0103245].

[40] The data used have been extracted from the PPDS acessible at http://pdg.lbl.gov (computer readable data files).

[41] M. Klein. *Status Report on THERA Studies*, to appear in the proceedings of the DIS2000 Conference, Liverpool (2000), [Available at THERA home page http://www.ifh.de/thera/].

[42] A.L. Ayala, M.B. Gay Ducati, E.M. Levin, Phys. Lett. **B388**, 188 (1996).

[43] E. Gotsman et al., *High density QCD at THERA*, [hep-ph/0101344].